

Correspondences between parameters in a reaction-diffusion model and connexin functions during zebrafish stripe formation

Akiko Nakamasu (✉ nakamasu@kumamoto-u.ac.jp)

Kumamoto Univ.

Article

Keywords: Pattern formation, Turing pattern, mathematical model, Reaction-diffusion system

Posted Date: July 14th, 2021

DOI: <https://doi.org/10.21203/rs.3.rs-658862/v2>

License:  This work is licensed under a Creative Commons Attribution 4.0 International License.

[Read Full License](#)

Version of Record: A version of this preprint was published at Frontiers in Physics on January 18th, 2022.
See the published version at <https://doi.org/10.3389/fphy.2021.805659>.

1 Title; Correspondences between parameters in a reaction-diffusion
2 model and connexin functions during zebrafish stripe formation.

3 Running Head; Link between experimental and theoretical Turing patterns

4 Akiko Nakamasu*

5 International Research Organization for Advanced Science and Technologies, Kumamoto

6 University, 2-39-1 Kurokami, Chuo-Ku, Kumamoto, 860-8555 Japan

7 * Corresponding author

8 **Email:** nakamasu@kumamoto-u.ac.jp

9 **Keywords**

10 Pattern formation, Turing pattern, Mathematical model, Reaction-diffusion system.

11

1 **Statements**

2 I had read and understood your journal’s policies, and believe that neither the
3 manuscript nor the study violates any of these, as follow. Data can be provided on request.

4 This research was supported by Grant-in-Aid for Scientific Research on Innovative Areas
5 (Japan Society for the Promotion of Science), Periodicity, and its modulation in plants.

6 No.20H05421. There are no conflicts of interest to declare. This study is not related to the
7 ethics approval and patient consent statement. Then the manuscript including pictures from

8 Usui et al. (2019) *Development* **146**, dev181065 in Fig.4 and Fig. 6. The use of the pictures
9 was permitted by the author M. Watanabe.

10

1 **Key Findings**

2 • An experimentally derived mathematical model could be applied to experimental
3 results published since the original development of the model.

4 • The terms of the mathematical model could be connected with the functions of
5 molecular channels on different cells.

6 • The model used partial differential equations (PDEs) enabled numerical and
7 mathematical analyses of characteristics observed in the experiments.

8 • Further improved PDE model including nonlinear reaction terms, enabled the
9 consideration of the behavior of components.

10

1 **Abstract**

2 Different diffusivities among interacting substances actualize the potential
3 instability of a system. When these elicited instabilities manifested as forms of spatial
4 periodicity, they are called Turing patterns. Simulations using general reaction-diffusion
5 (RD) models have demonstrated that pigment patterns on the body trunk of growing fish
6 follow a Turing pattern. Laser ablation experiments performed on zebrafish revealed
7 apparent interactions among pigment cells, which allowed for a three-components RD
8 model to be derived. However, the underlying molecular mechanisms responsible for
9 Turing pattern formation in this system had been remained unknown. A zebrafish mutant
10 with a spotted pattern was found to have a defect in Connexin41.8 (Cx41.8) which,
11 together with Cx39.4, exists in pigment cells and controls pattern formations. Here,
12 molecular-level evidence derived from connexin analyses was linked to the interactions
13 among pigment cells described in previous RD modeling. Channels on pigment cells were
14 generalized as “gates,” and the effects of respective gates were deduced. The model used
15 partial differential equations (PDEs) enabled numerical and mathematical analyses of
16 characteristics observed in the experiments. Furthermore, the improved PDE model
17 including nonlinear reaction terms enabled the consideration of the behavior of
18 components.

1 Introduction

2 In 1952, Alan Turing postulated that two substrates interacting with each other
3 show instability when they diffuse at different speeds. He explained this diffusion-driven
4 instability by utilizing a linear reaction-diffusion (RD) model. This model demonstrated that
5 spatial inhomogeneity (i.e., Turing pattern) could be generated by such conditions.¹ This
6 relationship is known to generate patterns, though the components remain to be explored.

7 More than two decades ago, Kondo and Asai (1995) reported that pigment
8 stripes on the bodies of growing marine angel fish behaved as a Turing pattern.² Research
9 focus then shifted mainly to zebrafish (*Danio rerio*) as a model organism for pattern
10 formation studies.^{3, 4, 5} Zebrafish have a pattern of stripes on their body and fins (Fig. 1A).
11 The pattern is generated by three types of pigment cells: complementarily distributed black
12 melanophores and yellow xanthophores (Fig. 1C), plus iridescent iridophores. Numerous
13 zebrafish pigment-pattern mutants were artificially generated⁶ and the corresponding genes
14 were identified. One of the most important mutants is *leopard*, which produce a spotted
15 pattern, that is representative of Turing patterns (Fig. 1B). Watanabe *et al.* (2006) identified
16 *connexin41.8* (*cx41.8*) as the gene responsible for the *leopard* mutation.⁷ Besides Cx41.8,
17 other connexins such as Cx39.4 exist in pigment cells and affect pigment-pattern formation.
18 Six connexins form a hemi-channel (or “connexon”), which connects intracellular and

1 extracellular spaces (Fig. 1D). Docking of two hemi-channels from adjacent cells give rise
2 to a gap junction, which mediates intercellular signal transfer.⁸ The minimal connexin
3 network required to originate a striped pattern was recently revealed by regulating connexin
4 expression in each pigment cell.⁹ Therefore, these channels are important for pigment-
5 pattern formation.

6 Interactions among pigment cells and their molecular mechanisms involved in
7 pattern formation are summarized in Volkening (2020).¹⁰ However, the molecular
8 mechanisms leading to Turing instability have remain mostly unresolved. Mosaic fish
9 experiments have indicated that both *leopard/cx41.8* and *jaguar/obelix/kcnj13* genes are
10 required for segregation of melanophores and xanthophores. Such segregation was
11 proposed to involve local interactions between adjacent pigment cells.¹¹ Xanthophore
12 ablation using a temperature-sensitive *csf1ra* allele led to the gradual death of
13 melanophores in both the body trunk and fins of adult fish.¹² Accordingly, melanophore
14 survival requires continuous signaling from xanthophores. Laser ablation of stripe and inter-
15 stripe areas has revealed the mutual interactions between melanophores and
16 xanthophores.¹³ The interactions comply with the requirements for Turing pattern formation
17 (Fig. 1E). Specifically, both types of pigment cells activate their own types at a single-cell
18 distance (short range) by inhibitions of other types, but then inhibit their own types beyond

1 the width of the stripe (long range). The difference in reaction distances achieves the “local
2 activation and lateral inhibition” condition needed for pattern formations.¹⁴ It should be
3 noted, however, that the distinction between iridophores and xanthophores was sometimes
4 unclear in those experiments.

5 To explain the opposing actions at long vs. short distance, a model that included
6 a highly diffusible molecule (i.e., long-range factor) and two cells (regarded as short-range
7 factors with low diffusivity) was constructed.¹³ This three-component RD model, with its
8 linear reaction terms and upper and lower limits, described the apparent interactions
9 obtained experimentally. Then the different diffusibilities and the interactions in the model
10 achieved diffusion-driven instability (Turing instability).

11 Further investigations revealed that the interactions were mediated by cell
12 projections.¹⁵ The interaction mediated by gap junctions on the tip of the projection was
13 considered to be a long-range effect observed in the previous experiments.¹⁶ The
14 researchers mentioned the possibility that the pattern formation might not require actual
15 diffusion. Later a Turing model based on an integral kernel was suggested,¹⁷ though the
16 link between parameter and molecular function was ambiguous. Most other models for the
17 pigment-pattern formation are based on interactions at a cellular level. These models
18 implemented different effects depending on the distance from each pigment cell.^{18, 19, 20}

1 Several attempts were made to explain the observed patterns in zebrafish mutants by a
2 general Turing model,^{21, 22} however, they were not supported experimentally, even though
3 there are several paths to cause the expected pattern changes in mutants.

4 Here, the interactions in a three-component model, including a highly diffusible
5 factor, were developed to attempt to link the molecular functions of connexins in zebrafish.
6 Channels thought to be important for the pattern formation were generalized as “gates” of
7 pigment cells. These gates enable transport of the diffusible molecule across the
8 membrane. The parameters affected by each gate were deduced, then the effects on
9 pattern-selection and -size, were analyzed. Finally, the model was improved to an
10 analogous model with nonlinear terms. These models together enabled reasonable
11 explanations of detailed behavior of the components that related to the pattern formation.

12

1 Results

2

3 Linear reaction-diffusion model for pigment-pattern formation

4 Previous laser ablation experiments revealed that the presence of mutual
5 interactions between two types of pigment cells were necessary to generate Turing
6 patterns (Fig. 1E). A mathematical model was derived from these apparent interactions in
7 Nakamasu *et al.* (2009),¹³ although the details of the relationship between the experimental
8 results and the model were not described. This model was based on the following set of RD
9 equations:

$$\begin{cases} \frac{\partial u}{\partial t} = D_u \nabla^2 u + f(v, w) - d_u u \\ \frac{\partial v}{\partial t} = D_v \nabla^2 v + g(u, w) - d_v v \\ \frac{\partial w}{\partial t} = D_w \nabla^2 w + h(u, v) - d_w w \end{cases} \quad (1)$$

10 Here the alternative distribution of two types of pigment cells (Fig. 1C) was
11 expressed by two factors (U, V) of the three components. Then u , and v was each volume
12 (viability). Numerical simulation of this model resulted in a Turing pattern in which u and v
13 were distributed with antiphase while a concentration of third factor W (w), presented
14 peaks synchronized with u (Fig. 2). It should be noted that cell divisions of differentiated
15 melanophores contribute only minimally to the pigment-pattern formation in fish (Fig. 1F).

1 Therefore, the number of melanophores is changed by 1) supply of new cells from
2 randomly scattered precursor cells, 2) death of existing pigment cells, or 3) migration from
3 a position close to the skin surface.²³ In the case of melanophores, it is known that cell
4 movements and cell deaths are complementary to each other.²⁴ Even though they are
5 inhibited, xanthophores are found in the stripe region, where they exist with a pale color.²⁵
6 ^{26,27} Xanthophores do not move actively *in vivo*, as may be the case for iridophores. As
7 detailed in Fig. 1F, motilities of the cells were approximated by small diffusion coefficients
8 (D_u and D_v). The rapidly diffusing factor W was assigned a large diffusion coefficient
9 (D_w).

10 The parameters in the reaction formulae were positive constants as shown in
11 Table 1. Each formula was composed of a set of linear terms with upper and lower limits as
12 follows:

$$\left\{ \begin{array}{l} f(v, w) = \begin{pmatrix} 0; -i_{uv}v - i_{uw}w + s_u < 0 \\ -i_{uv}v - i_{uw}w + s_u; 0 < -i_{uv}v - i_{uw}w + s_u < f_{max} \\ f_{max}; -i_{uv}v - i_{uw}w + s_u > l_{max} \end{pmatrix} \\ g(u, w) = \begin{pmatrix} 0; -i_{vu}u + p_{vw}w + s_v < 0 \\ -i_{vu}u + p_{vw}w + s_v; 0 < -i_{vu}u + p_{vw}w + s_v < g_{max} \\ g_{max}; -i_{vu}u + p_{vw}w + s_v > m_{max} \end{pmatrix} \\ h(u, v) = \begin{pmatrix} 0; p_{wu}u - c_{wv}v + s_w < 0 \\ p_{wu}u - c_{wv}v + s_w; 0 < p_{wu}u - c_{wv}v + s_w < h_{max} \\ h_{max}; p_{wu}u - c_{wv}v + s_w > n_{max} \end{pmatrix} \end{array} \right. \quad (2)$$

13 The cells were assumed to be inhibiting mutually ($-i_{uv}$, $-i_{vu}$), then W was
14 assumed to be produced by U (p_{wu}) and consumed by V ($-c_{wv}$). Accordingly, W was

1 assumed to inhibit pigment cells of the producer ($-i_{uw}$) and produce (or preserve) the
2 consumer (p_{vw}). The self-coupling parameters $-d_u$, $-d_v$, $-d_w$ corresponded to
3 degradation (or death) coefficients, whereas s 's represented constants related to supply
4 (also called "support sustainability") of each component. The producer U activated V , but
5 then inhibited itself at long range via W . By consuming W , V also indirectly inhibited itself,
6 but then was activating U by double inhibition at long range. As a result, U and V
7 exhibited no difference in apparent interactions, making it difficult to identify which factor
8 corresponded to which cell type. Besides melanophores, xanthophores also showed self-
9 inhibition at long range. In laser ablation experiments, melanophore elimination in adjacent
10 stripes caused pale-colored xanthophores in an inter-stripe region. Therefore, the pale
11 color reflects xanthophore inhibition even without a change in cell number.

12 The three-component model in (1) is somewhat complex, though it can be applied
13 to a combination of two-variable systems as follows.

$$\begin{cases} \frac{\partial x}{\partial t} = f_x x + f_y y + D_x \nabla^2 x \\ \frac{\partial y}{\partial t} = g_x x + g_y y + D_y \nabla^2 y \end{cases} \quad (3)$$

14 There are two different cases that bring diffusion driven instabilities, i.e., activator-
15 inhibitor type (Fig. 3A) or activator-substrate-depletion type (Fig. 3B), characterized by

1 different signs of the parameters.^{28,29} Both conditions were included in the three-component
2 model (Fig. 3C). Therefore, each parameter in the model can be regarded as part of a two-
3 variable system. The first and second reaction formulae (2) include mutual inhibitions
4 $(-i_{uv}v, -i_{vu}u)$, each of which corresponds to the respective self-activation ($f_x > 0$ for x),
5 though it cannot be realized without each partner. Recent experiments revealed that
6 xanthophores are generated from division of other xanthophores.²⁷ Therefore, at least one
7 of self-reaction parameters; $-d$ for u or v in (2), cannot be a degradation coefficient, i.e.,
8 it might be a non-negative parameter.

9

10 **Effects of the parameters on the component proportion and the characteristic**
11 **wavelength of a pattern.**

12 Variation in patterns observed in most zebrafish mutants is explained by
13 changes in the types and sizes of patterns. The former is defined by pattern selection,^{30,31}
14 and manifests as a general variation of the Turing pattern from spots, to stripes to reverse
15 spots. The latter is dictated by the characteristic wavelength of the pattern.³² The following
16 sections analytically describe the effect of parameters in the model (1)-(2) on these
17 characteristics.

1 ***Effects of parameter on pattern size***

2 The characteristic wavelength of a pattern can be analytically derived from the
3 dispersion relation of linear stability.³² The wavelength of a two-variable RD system (3) is
4 given by the following equations:

$$\frac{2\pi}{k_{max}} = \sqrt{\frac{\sqrt{D_x D_y} (D_y - D_x)}{(D_x + D_y) \sqrt{-f_y g_x} - \sqrt{D_x D_y} (f_x - g_y)}} \quad (4)$$

5 k_{max} is a preferable wave number in a system. As mentioned above, each
6 parameter in the model can be regarded as a two-variable system (Fig. 3C). The mutual
7 inhibitions ($-i_{uv}v$, $-i_{vu}u$) correspond to the self-activation, though they are inversely
8 related, i.e., the sign of the parameters is different from f_x in two-variable systems. The
9 increase in the absolute values of the parameters reinforces the self-activation. At the same
10 time, the effects of $-d_u$ and $-d_v$ are opposite of f_x . The effect on pattern size when the
11 absolute value of each parameter is decreased (i.e., the decline of each interaction) is
12 shown in Fig. 2D and indicates correspondence with two-variable systems (Fig. 3A, B).

13 ***Effects of parameter on pattern selection***

14 In zebrafish, pattern selection is determined mainly by the proportion of two
15 types of pigment cells with complimentary distribution. The relative position of the

1 equilibrium from the limits of the reaction terms provides an index for pattern selection,³¹ as
2 that is the origin of diffusion-driven instability.

3 Considering differential equations of the volume of two cells (u and v), the
4 decrease in each absolute value (i.e., the decline of each interaction) of the parameter with
5 a positive effect decreases the population volume of respective cells, then that of the
6 parameter with a negative effect increase the population of the respective cells. Here, the
7 component W with high diffusivity represses u and promotes v , therefore, the decrease
8 in the positive parameter in the differential equations of w increases u and decreases v
9 respectively. The opposite can apply to negative parameters. From this aspect, however, it
10 is difficult to refer about the combined effect of parameters with different signs.

11

12 **Correspondence between the mathematical model and connexin defects in zebrafish** 13 **estimated from molecular function**

14 Next, correspondence between this model and molecular functions was
15 assumed (Fig. 1G). In zebrafish, *leopard* mutants are known to have an aberrant pigment
16 pattern, whereby stripes are changed to spots³³ (Fig. 1A, B). The gene responsible for the
17 *leopard* mutation is a connexin *cx41.8*, which encodes a four trans-membrane connexin

1 protein. Additionally, mutation of connexin *cx39.4* results in wavy stripes. Recent analyses
2 of connexin activity have revealed different functions associated with hemi-channels and
3 gap junctions.^{34, 35} Hemi-channels are open to the extracellular environment, whereas gap
4 junctions form connections between cells to allow the exchange of small molecules (Fig.
5 1D). Accordingly, connexins may be involved in both long- and short-range interactions.
6 These channels may function as gates for the transport of molecule W across the
7 membrane (Fig. 1G). Accordingly, producer U produces W , which then diffuses outside
8 the cell into the extracellular space via some kind of gate. Therefore, gate defects affect
9 survival of the producer by preventing release of harmful W (i. e., d_u of $-d_u$ is
10 increased). I considered two other possibilities, i.e., the effect of gate defect on D_w and/or
11 i_{uw} . If D_w was changed, W outside of the cells will also be affected. A u -dependent
12 decrease in D_w might be more appropriate for the assumption of enclosed W . Though, it
13 will give difficulties in the analytical approach and both will finally result in an increase in the
14 death of U . Then the degree of harmful effect on U by same concentration of W would not
15 change. Therefore, D_w and i_{uw} would not be affected. w had peaks with the peaks of
16 producer U and gates on cells assumed passive effects on W movements. This explain
17 why p_{wu} might not be affected, at least directly. Consumer V was assumed to incorporate
18 beneficial W into the cell across the gates then to consumes it, indicating that the gate

1 defects will decrease the parameters c_{vw} of $-c_{vw}$ and p_{wv} . Both parameters were
2 assumed to be related to intracellular events, therefore, higher w was needed for the
3 same rate of consumption and V production compared with the case of intact hemi-
4 channels. At the same time, parameters for mutual inhibitions i_{uv} and i_{vu} are decreased
5 by the *leopard* mutation,³⁶ through gap junctions (combination of gates) at short range.
6 They would be simultaneously affected linking with the hemi-channel defect on the
7 corresponding cell. In Fig.1G, these parameters linked to different gates are indicated by
8 different hatchings.

9

10 **Comparisons of results obtained by simulation and experiments.**

11 First, the independent effects of the gate on each cell were analyzed numerically.
12 When an arbitrary stripe is set as a starting point, only gates that opened to the outside on
13 U and V cells were removed along the x- and y-axes. Numerical simulation of this model
14 yielded a spot pattern of u in the case where gates on U cells had defects, as expected
15 by the sign of the parameter (Fig. 4A). Reversed u spots were yielded in V cell defects
16 (Fig. 4B), though the change was not strong, because it included opposite effects on V
17 volume. Pattern simplicity score (PSS) increased in both cases, then overall color tones

1 (OCT) were decreased and increased by respective defects. That is, the asymmetry of
2 changes in pattern selection can be observed by the removals of gates on respective cell
3 types.

4 Defects on short-range inhibition did not have drastic effects on pattern selection,
5 though the pattern did finally disappear (Fig. 4C). On the 2D plane, the stripe region was
6 recessive together with the defect in short-range effects by gap-junctions (Fig. 4D-H, J),
7 though the tendency to shift the pattern selection was not changed. In Fig. 4I, short-range
8 effects were simultaneously decreased by respective x or y values that linked with U or
9 V defects, as shown in right panel in Fig. 4J. This also kept the same tendency to shift the
10 pattern selection with individual cases.

11 The results mostly consisted with the positive effects of connexin additions to
12 WKO that increased the respective pigment cells.⁹ However, experimental eliminations of
13 gate on each wild-type pigment cell led to an increase in the rate of respective pigment
14 cells; melanophore defects generated net patterns of melanophores, while the xanthophore
15 defects resulted in dot patterns of melanophores (i.e., net patterns of
16 xanthophore). Therefore, the simulation results were partly inconsistent with experimental
17 results in Usui *et al.* (2019),⁹ in which the effects of connexins on each or both pigment
18 cells were investigated in detail (Fig. 4K).

1 From the electro-physiological experiments in Watanabe *et al.* (2016),³³ each
2 type of connexin could be considered to have different strengths of the (hemi-) channel
3 functions on the two types of cells. Deduced patterns of respective transgenic fishes were
4 indicated by small letters on the phase plane in Fig. 4I. Even though the differences in the
5 strengths of channels were taken account, the removal of hemi-channels on wild-type
6 xanthophores tended to increase the population of xanthophore then a faint increase in
7 melanophores was brought in the case of connexin on melanophores (Fig. 4K). If cell U is
8 a melanophore, other than the gray-framed patterns shown in Fig. 4K did not seem to
9 correspond to Fig 4I, though all of the experimentally obtained patterns are existed in the
10 simulation. As describe more distinctly, some shuffles can give a strong correspondence
11 with Fig. 4I (Fig. 6).

12 From the analyses of wavelength mentioned above, defects to the gates on cell U
13 (increasing in d_u of $-d_u$) or cell V (decreasing in p_{vw} and c_{wv}) caused a decrease or an
14 increase in pattern size, respectively. In numerical simulations, the pattern size tended to
15 be decreased and increased by the hemi-channel defects on both U and V cells, as
16 expected (Fig. 3A, B). The characteristic thinning of u stripes and widening of v inter-
17 stripes were observed in the simulation of U -cell defects, though it was not explained by
18 the analyses. From the characteristic thinning of the u stripe, each cell corresponding to

1 one of two short-range factors may be deduced. However, the thinning was observed on
 2 melanophore stripe, in the case of defect in xanthophore. Inconsistent with the U defect,
 3 melanophore defect tented to result in wide melanophore stripes in the experiment.

4

5 **Non-linearization of the model**

6 To describe the behavior of the components in the system in greater detail, the
 7 model was non-linearized. As an example, we devised a model with nonlinear terms as
 8 shown in (5), though qualitative relationships were not changed from the model shown in
 9 Fig 1F.

$$\begin{cases} \frac{\partial u}{\partial t} = D_u \nabla^2 u - i_{uv} uv - i_{uw} uw + d_u u + \frac{s_u}{1 + u + v} \\ \frac{\partial v}{\partial t} = D_v \nabla^2 v - i_{vu} vu + p_{vw} vw - d_v v + \frac{s_v}{1 + u + v} \\ \frac{\partial w}{\partial t} = D_w \nabla^2 w + p_{wu} u - c_{wv} wv - d_w w + s_w \end{cases} \quad (5)$$

10 This model, using nonlinear RD equations, also generated Turing patterns (Fig.
 11 5). Considering interactions between different types of cells and between cells and
 12 molecules, inhibitions were given by multiplication terms (e.g., the inhibition of U by W
 13 was described as uw , and so on). These multiple terms are based on the description of
 14 second-order reaction in chemical kinetic equation or dimer reactions by Meinhardt

1 (1982),³⁷ it enabled only limited reaction by the contacts between the components. W was
 2 needed for maintenance of cell V so this reaction was also given by a multiplication term
 3 of their volume. On the other hand, production of W by U will only occur u -dependently,
 4 and degradation (and deaths) will also be w -dependent. Therefore, those terms are linearly
 5 related to each component. These non-linearizations can identify the actions on an existing
 6 cell or a newly differentiating cell. Then new generations of pigment cells occur only with
 7 eliminations of existing cells.³⁸ Therefore, mature cells would inhibit the generation of cells.
 8 The sign of d_u seemed prefer to be positive for the start point of pattern selection
 9 corresponded to zebrafish i.e., the start from stripe. Even though the sign was opposite to
 10 the linear model, total u change may become minus with relation to other components
 11 (i.e., $-i_{uv}v - i_{uw}w + d_u < 0$ in the deformed reaction terms $(-i_{uv}v - i_{uw}w + d_u)u +$
 12 $s_u/(1 + u + v)$). Therefore, the self-productivity can be small enough to agree with the low
 13 proliferation rate of melanophores. Similar, concerns about the self-productivity of
 14 xanthophores mentioned above, $\partial v/\partial t$ in (5) already had a self-productivity by the
 15 multiplication term vw , regardless of the sign of d_v (i.e., $-i_{vu}u + p_{vw}w - d_v > 0$ in
 16 deformed reaction terms $(-i_{vu}u + p_{vw}w - d_v)v + s_v/(1 + u + v)$). The sign of d_v can be
 17 inverted though the change were not expected to substantially affect pattern
 18 characteristics.

1 Next, numerical calculations of the nonlinear model were performed to consider
2 the condition where respective gates on U and V cells, and both-gate defects were added
3 (Fig. 5A-C). Again, numerical results consistent with linear model could be obtained from
4 an arbitrary parameter set generating a stripe pattern. Biased pattern shift could also be
5 obtained by simulations, partly corresponding to connexin-mutation experiments. When
6 gates on U cell were deleted, it resulted in a u dot pattern (Fig. 5A). Simultaneous
7 decreases in p_{vw} and c_{wv} by increasing the gate defect on V cells generated a net of u ,
8 though not so drastic (Fig. 5B). Defect in gap-junction by decreasing i_{vu} and i_{uv} , had
9 minimal effect, though the stripe region became recessive with combination of defects on
10 each outer gate (Fig. 5C, D). The thinning of the u population was not clear because of the
11 thin stripe at the start.

12

1 Discussion

2 In the present study, to confirm the potency of diffusion-driven instability in
3 determining fish pigmentation patterns, channels on pigment cells were generalized as
4 “gates” (Fig. 1). The three-component RD model (1) was shown to be composed of two-
5 variable RD systems bringing diffusion driven instabilities (Fig. 2, 3). The proposed
6 qualitative models help to understand the relationship between pigment cells, as well as
7 between cells and molecules, even when their identity is unknown. The terms of the
8 theoretical model were connected with the functions of each channel on different cells.
9 Parameters affected by the gate defects were deduced (Fig.1G) then the effects of such
10 defects were simulated from a parameter set that generated an arbitrary stripe as a
11 benchmark (Fig. 4, 5). Then, dots and thinning of the U cell population could be obtained
12 by a defect of the gate on it in numerical simulations. The identities of melanophores and
13 xanthophores were deduced from the change of pattern selection and the wavelengths,
14 though the identify of important substance W is still missing. Then, improvements to the
15 nonlinear model enabled a description of the detailed behaviors of components that are
16 related to the pattern formation. Though the numerical analyses could not strictly explain
17 the pattern obtained by experimental manipulation of connexins by Usui *et al.* (2019),⁹ the

1 present study can help to interpret the mechanism underlying the *leopard* mutation, as a
2 Turing system.

3 The determinations of the signs of self-reaction terms for U and V were difficult.
4 The signs of d_u prefer to invert for a desirable range of pattern selection start from stripe in
5 the improved nonlinear model, though the total changes for U (= melanophore)
6 corresponded to experimental observations. The increase in existing melanophores
7 brought by positive d_u were visible by the laser ablation of adjacent xanthophores or
8 deletion of stripes in the experiments in Nakamasu *et al.* (2009),¹³ Each manipulation
9 decreased $-i_{uv}vu$ or $-i_{uw}wu$ inhibitions, respectively. On the other hand, the self-
10 productivity of xanthophores in the nonlinear model can be achieved even though the
11 negative coefficient of self-reaction. The combination of two-cases of diffusion driven
12 instability in the three-component model indicates the capacity to make a pattern without
13 melanophore by the self-productivity of xanthophore, if sufficient W is added externally.
14 On the other hand, if melanophores have strong self-productivity, it will also be able to
15 make a pattern without xanthophores by the removal of extra W .

16 Connexins are related to both hemi-channels and gap junctions. Hemi-channels
17 have been considered less important in physiology, although it was recently revealed that
18 the aberrant activity of hemi-channels could change the proportion of vertebrae³⁴ and was

1 related to the pigment-pattern formation in zebrafish^{33,35} Laser ablation experiments
2 showed that the interactions between xanthophores and melanophores differed depending
3 on the distance. In the present model, the highly diffusible molecule W had a positive
4 effect on V . Hence, the inhibition of V via gap junctions is inconsistent. Outflow of harmful
5 W from U via gap junctions is also inconsistent with the inhibition. This elicits a different
6 signal transduction cascade as cell depolarization³⁹ and incorporation of functions for
7 molecules other than connexin should be envisioned. Then the inverted function may be
8 derived from an observed rectified current in gap junction. It was observed that quail
9 melanocytes interacted with each other via filopodia *in vivo* and *in vitro*.⁴⁰ Gap junctions
10 may have functions on interactions not only between other types of cells but among the
11 same populations. Though, the obtained simulation results included several collisions with
12 experimental results. Similar discords were also in experiments. The results of Usui *et al.*
13 (2019)⁹ indicated that either Cx41.8 or Cx39.4 is needed on melanophores then Cx41.8 is
14 necessary and sufficient on xanthophore for (stripe) pattern formation. However, such
15 “necessary and sufficient” trait for aberrant currents could be observed in hemichannels
16 composed of Cx39.4 in the absence of calcium, in electro-physiological experiments.³³
17 Shuffle of mutant fish further supported the numerical results shown in Fig. 6. In this case,

1 expected Cx41.8 manipulations showed the “necessary and sufficient” trait on
2 melanophores.

3 Similar effects of connexin mutations (i.e., shift from stripe to dots) can be
4 observed both on the body and fins. Because of the fins lack iridophores, the effect on the
5 pigment pattern formation depends on the relationship between melanophores and
6 xanthophores. Even though pattern formation is achieved by the two types of cells, details
7 on the role of iridophores in cellular interactions have been revealed.¹¹ The evaluation of
8 the iridophore function in similar modeling will also be possible and should be attempted.

9 Using such a model with partial differential equations will lead to various
10 mathematical analyses. For example, pattern size was mathematically analyzed with
11 regard the model as combination of two-variable systems here. This method cannot yet
12 describe the independent pattern sizes of each type of pigment cell that have been
13 observed experimentally²² and predicted numerically. Therefore, more sophisticated
14 analyses will be required in the future.

1 **Materials and Methods**

2 **Numerical simulations**

3 For the linear model, d_u was increased from 0 to 0.2 within limits along the x -axis
4 (Fig. 4A, D-H) and the parameters p_{vw} and c_{wv} were decreased linearly from 1 to 0 (Fig.
5 4B, D-H) for investigation of the effect of gates on each cell. For short-range effects, i_{uv}
6 and i_{vu} were decreased linearly from 1 to 0.6 in Fig. 4C. Accordingly, the arbitrary
7 parameter set generating stripes (wild-type) was placed in the right top of the phase plane
8 (Fig. 4D-I). Partial differential equations were calculated with 20000 and 40000 iterations
9 with $dt = 0.1$ and $dt = 0.05$, in fields sized $xl = 56.25$, $yl = 225$ with $dx = 0.75$ and $xl =$
10 $yl = 200$ with $ds = 0.5$ for Fig. 3A-C and Fig. 3D-H, respectively. In Fig. 4I, to investigate
11 the simultaneous gap-junction effects with hemi-channels $s_d(x, y) = 1 - 0.002 \max\{x, y\}$,
12 $u_d(x) = 0.0004x$, and $v_d(y) = 1 - 0.002y$ were utilized in the field sized $x = y = 300$
13 ($dx = 0.75$) and $dt = 0.1$ for 20000 iterations.

14 For the non-linear model, the parameters d_u , and i_{uv} and i_{vu} were decreased
15 linearly from 1 to 0.6. c_{wv} and p_{vw} were decreased linearly from 0.5 to 0.1 in Fig. 5 A-C,
16 and decreased by $s_d(x, y) = 1 - 0.002 \max\{x, y\}$ simultaneously in Fig. 5D. Accordingly,
17 the arbitrary parameter set generating stripes (wild-type) was placed in the right top of the
18 phase plane. Partial differential equations were calculated in fields sized $xl = 10$, $yl = 40$

1 in Fig. 5A-C and $xl = yl = 50$ with $ds = 0.25$ in Fig. 5D. Then after 500000 iterations
2 calculated with $dt = 0.01$, we obtained the result.

3 Calculations were performed in the language Full BASIC with no-diffusion boundary
4 conditions then and results are shown as density plots of u . Parameters utilized in this
5 study are summarized in Table 1.

6

7 **Quantification of color patterns**

8 Color pattern complexity and overall tone were quantified from binarized images using the
9 ImageJ as described in Miyazawa *et al.* (2010).⁴¹ Briefly, the pattern simplicity score (PSS)
10 is defined as the area weighted mean isoperimetric quotient of the contours extracted from
11 each image. The overall color tone (OCT) of a pattern is defined and calculated as the ratio
12 of white pixels in the binarized image. Analyzed images were prepared by the quaternary
13 connection of a numerical result (100×100 individual fields with periodic boundary
14 conditions) of u in each parameter.

15

1 **References**

- 2 1. Turing AM. The chemical basis of morphogenesis. *Philos Trans R Soc Lond B*. 1952;
3 462: 27-73.
- 4 2. Kondo S, Asai R. A reaction-diffusion wave on the skin of the marine angelfish
5 Pomacanthus. *Nature*. 1995; 376: 765-768.
- 6 3. Johnson SL, Africa D, Horne S, Postlethwait JH. Half-tetrad analysis in zebrafish:
7 Mapping the ros mutation and the centromere of linkage group I. *Genetics*. 1995a;
8 139: 1727-1735.
- 9 4. Johnson SL, Africa D, Walker C, Weston JA. Genetic control of adult pigment stripe
10 development in zebrafish. *Dev Biol*. 1995b; 167: 27–33.
- 11 5. Kelsh RN. Genetics and evolution of pigment patterns in fish. *Pigment Cell Res*.
12 2004; 17: 326-336.
- 13 6. Haffter P, Granato M, Brand M, Mullins MC, Hammerschmidt M, Kane D, Odenthal
14 J, van Eeden FJ, Jiang YJ, Heisenberg CP, Kelsh R N, Furutani-Seiki M, Vogelsang
15 E, Beuchle D, Schach U, Fabian C, Nüsslein-Volhard C. The identification of genes
16 with unique and essential functions in the development of the zebrafish, *Danio rerio*.
17 *Development*. 1996; 123: 1-36.
- 18 7. Watanabe M, Iwashita M, Ishii M, Kurachi Y, Kawakami A, Kondo S, Okada N. Spot

- 1 pattern of *leopard* Danio is caused by mutation in the zebrafish connexin41.8 gene.
2 *EMBO reports*. 2006; 7: 893-897.
- 3 8. Kumar NM, and Gilula NB. The gap junction communication channel. *Cell*. 1996; 84:
4 381-388.
- 5 9. Usui Y, Aramaki T, Kondo S, Watanabe M. The minimal gap-junction network among
6 melanophores and xanthophores required for stripe-pattern formation in zebrafish.
7 *Development*. 2019; 146: dev181065.
- 8 10. Volkening A. Linking genotype, cell behavior, and phenotype: multidisciplinary
9 perspectives with a basis in zebrafish patterns. *Curr Opin Genet Dev*. 2020; 63: 78-
10 85.
- 11 11. Maderspacher F, Nusslein-Volhard C. Formation of the adult pigment pattern in
12 zebrafish requires *leopard* and *obelix* dependent cell interactions. *Development*.
13 2003; 130: 3447-3457.
- 14 12. Parichy D, Turner J. Temporal and cellular requirements for Fms signal inducing
15 zebrafish adult pigment pattern development. *Development*. 2003; 130: 817-833.
- 16 13. Nakamasu A, Takahashi G, Kanbe A, Kondo S. Interactions between zebrafish
17 pigment cells responsible for the generation of Turing patterns. *Proc Natl Acad Sci U*
18 *S A*. 2009; 106: 8429-8434.

- 1 14. Meinhardt H, Gierer A. Application of a theory of biological pattern formation based
2 on lateral inhibition. *J Cell Sci.* 1974; 15: 132-146.
- 3 15. Hamada H, Watanabe M, Lau HE, Nishida T, Hasegawa T, Parichy DM, Kondo S.
4 Involvement of Delta/Notch signaling in zebrafish adult pigment stripe patterning.
5 *Development.* 2014; 141: 318-324.
- 6 16. Watanabe M, Kondo S. Fish pigmentation. Comment on "Local reorganization of
7 xanthophores fine-tunes and colors the striped pattern of zebrafish". *Science.* 2015;
8 348: 297.
- 9 17. Kondo S. An updated kernel-based Turing model for studying the mechanism of
10 biological pattern formation. *J Theor Biol.* 2017; 414: 120-127.
- 11 18. Bullara DW, De Decker Y. Pigment cell movement is not required for generation of
12 Turing patterns in zebrafish skin. *Nat Commun* 2015; 6: 6971.
- 13 19. Volkening A, Sandstede A. Iridophore as a source of robustness in zebrafish stripes
14 and variability in *Danio* patterns. *Nat Commun.* 2018; 9: 3231.
- 15 20. Owen JP, Kelsh RN, Yates CA. A quantitative modeling approach to zebrafish
16 pigment pattern formation. *Elife.* 2020; 9: E52998.
- 17 21. Asai R, Kondo S. Zebrafish *Leopard* gene as a component of the putative reaction-
18 diffusion system. *Mech Dev.* 1999; 89: 87-92.

- 1 22. Watanabe M, Kondo S. Changing clothes easily: connexin41.8 regulates skin pattern
2 variation. *Pigment Cell and Melanoma Res.* 2012; 25: 326-330.
- 3 23. Takahashi G, Kondo S. Melanophore in the stripe of adult zebrafish do not have the
4 nature to attract, but disperse when they have the space to move. *Pigment Cell and*
5 *Melanoma Res.* 2008; 21: 677-686.
- 6 24. Sawada R, Aramaki T, Kondo S. Flexibility of pigment cell behavior permits the
7 robustness of skin pattern formation. *Genes Cells.* 2018; 23: 537-545.
- 8 25. Hirata M, Nakamura K, Kanemaru T, Shibata Y, Kondo S. Pigment cell organization
9 in the hypodermis of zebrafish. *Dev Dyn.* 2003; 227: 497-503.
- 10 26. Hirata M, Nakamura K, Kondo S. Pigment cell distributions in different tissues of the
11 zebrafish, with special reference to the striped pigment pattern. *Dev Dyn.* 2005; 234:
12 293-300.
- 13 27. Mahalwar P, Walderich B, Singh AP, Nusslein-Volhard C. Local reorganization of
14 xanthophores fine-tunes and colors the striped pattern of zebrafish. *Science.* 2014;
15 345: 1362-1364.
- 16 28. Gierer A, Meinhardt H. A theory of biological pattern formation. *Kybernetics.* 1972;
17 12: 30-39.
- 18 29. Murray JD. *Mathematical Biology II.* Seattle, WA: University of Washington; 1989.

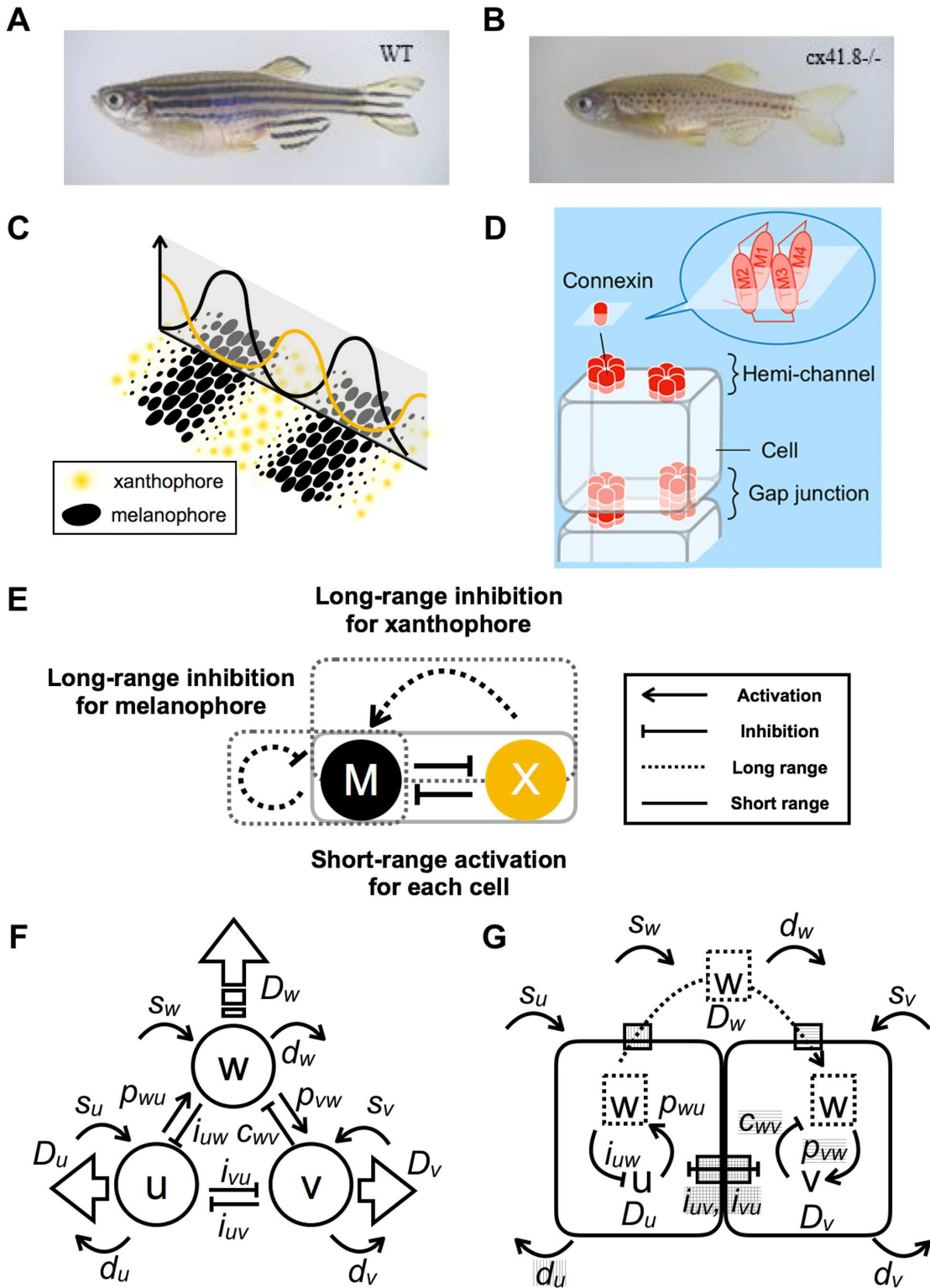
- 1 30. Ermentrout B. Stripes or spots? Nonlinear effects in bifurcation of reaction-diffusion
2 equations on the square. *Proc R Soc A*. 1991; 434: 1891.
- 3 31. Shoji H, Iwasa Y, Kondo S. Stripes, spots, or reversed spots in two-dimensional
4 Turing systems. *J Theor Biol*. 2003; 224: 339-350.
- 5 32. Miura T, Maini PK. Speed of pattern appearance in reaction-diffusion models:
6 Implications in the pattern formation of limb bud mesenchyme cells. *Bull Math Biol*.
7 2004; 66(4): 627-649.
- 8 33. Watanabe M, Sawada R, Aramaki T, Skerrett IM, Kondo S. The physiological
9 characterization of connexin41.8 and connexin39.4, which are involved in the striped
10 pattern formation of Zebrafish. *J Boil Chem*. 2016; 291: 1053-1063.
- 11 34. Misu A, Yamanaka H, Aramaki T, Kondo S, Skerrett IM, Iovine MK, Watanabe M.
12 Two different functions of connexin43 confer two different bone phenotypes in
13 zebrafish. *J Biol Chem*. 2016; 291: 12601-12611.
- 14 35. Watanabe M. Gap Junction in the Teleost Fish Lineage: Duplicated Connexins May
15 Contribute to Skin Pattern Formation and Body Shape Determination. *Front Cell*
16 *Dev Boil*. 2017; 5: 13.

- 1 36. Yamanaka H, Kondo S. In vitro analysis suggests that difference in cell movement
2 during direct interaction can generate various pigment patterns in vivo. *Proc Natl*
3 *Acad Sci U S A*. 2013; 111: 1867-1872.
- 4 37. Meinhardt H. In *Models of Biological Pattern Formation*. London: Academic Press;
5 1982: Chapter 11. Cell determination.
- 6 38. Yamaguchi M, Yoshimoo E, Kondo, S. Pattern regulation in the stripe of zebrafish
7 suggests an underlying dynamic and autonomous mechanism. *Proc Natl Acad Sci*
8 *U S A*. 2007; 104(12): 4790-4793.
- 9 39. Inaba M, Yamanaka H, Kondo S. Pigment Pattern Formation by Contact-Dependent
10 Depolarization. *Science*. 2012; 335: 677.
- 11 40. Inaba M, Jiang T-X, Liang Y-C, Tsai S, Lai Y-C, Widelitz RB, Chuong CM. Instructive
12 role of melanocytes during pigment pattern formation of the avian skin. *Proc Natl*
13 *Acad Sci U S A*. 2019; 116: 6884-6890.
- 14 41. Miyazawa S, Okamoto M, Kondo S. Blending of animal colour patterns by
15 hybridization. *Nat Commun*. 2010; 1071: 1-6.
16

1 **Acknowledgments**

2 The author would like to thank Masakatsu Watanabe and Masafumi Inaba for ~~persistent~~
3 stimulating discussions and important comments, as well as members of the Higaki lab. for
4 providing a suitable environment to concentrate on this investigation. I would also like to
5 thank Editage (www.editage.com) for English language editing and the IROAST
6 Proofreading/ Publication Support Program. This research was supported from Grant-in-Aid
7 for Scientific Research on Innovative Areas (The Japan Society for the Promotion of
8 Science), Periodicity and its modulation in plant No.20H05421 and Research grant from
9 Shimadzu Science Foundation.

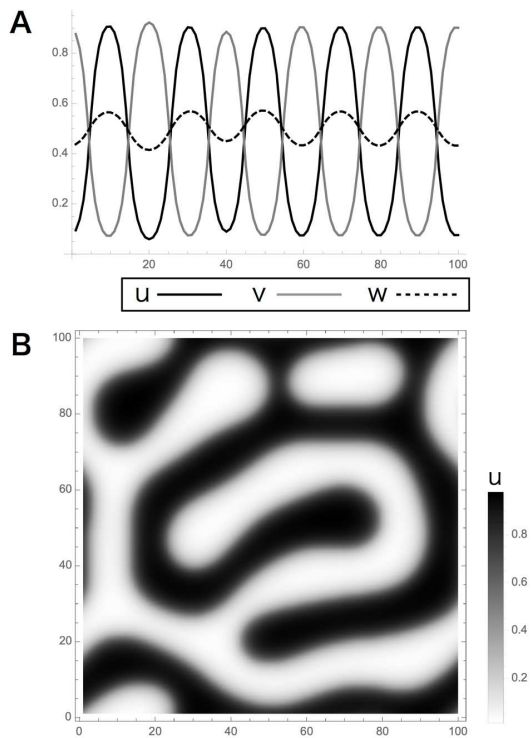
1 **Figures and Tables**



2

3 **Figure 1. Model-based prediction of defects in channels and interactions.**

1 (A) Striped wild-type (WT) zebrafish. (B) Spotted *leopard* mutant zebrafish. (C) Schematic
2 representation of the relationship between the distribution of pigment cells and the
3 numerical result of the continuous model. (D) Schematic representation of channels
4 composed of connexin complexes. Hemi-channels open to the outside of a cell, whereas
5 gap junctions formed by the docking of hemi-channel connect adjacent cells. (E) Apparent
6 interactions of pigment cells, as revealed by laser ablation experiments. (F) Schematic
7 diagram of a three-variable partial differential equation model composed of components U
8 or V , which correspond to melanophores or xanthophores, respectively, and component
9 w , which represents a highly diffusible molecule. Interactions are indicated by fine arrows,
10 diffusion coefficients (the motility of the components) are indicated by wide arrows, and
11 corresponding parameters are indicated. (G) Schematic diagram of the effect of channels
12 on pigment cells according to the mathematical model. Parameters related to the function
13 of each gate are indicated by hatchings.
14



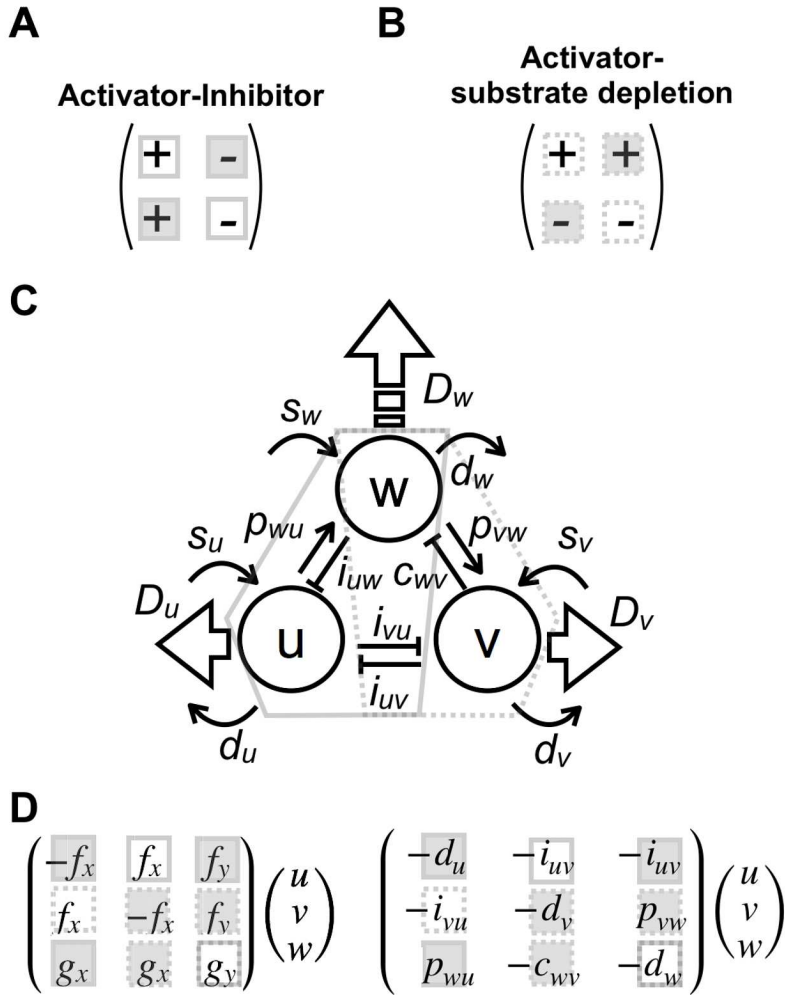
1

2 **Figure 2. Turing pattern obtained by applying a reaction-diffusion model.**

3 (A), (B) Calculation results of the model had linear terms with limits. (A) One dimension and

4 (B) two dimensions. Results indicate Turing patterns, in which the variables u and v are

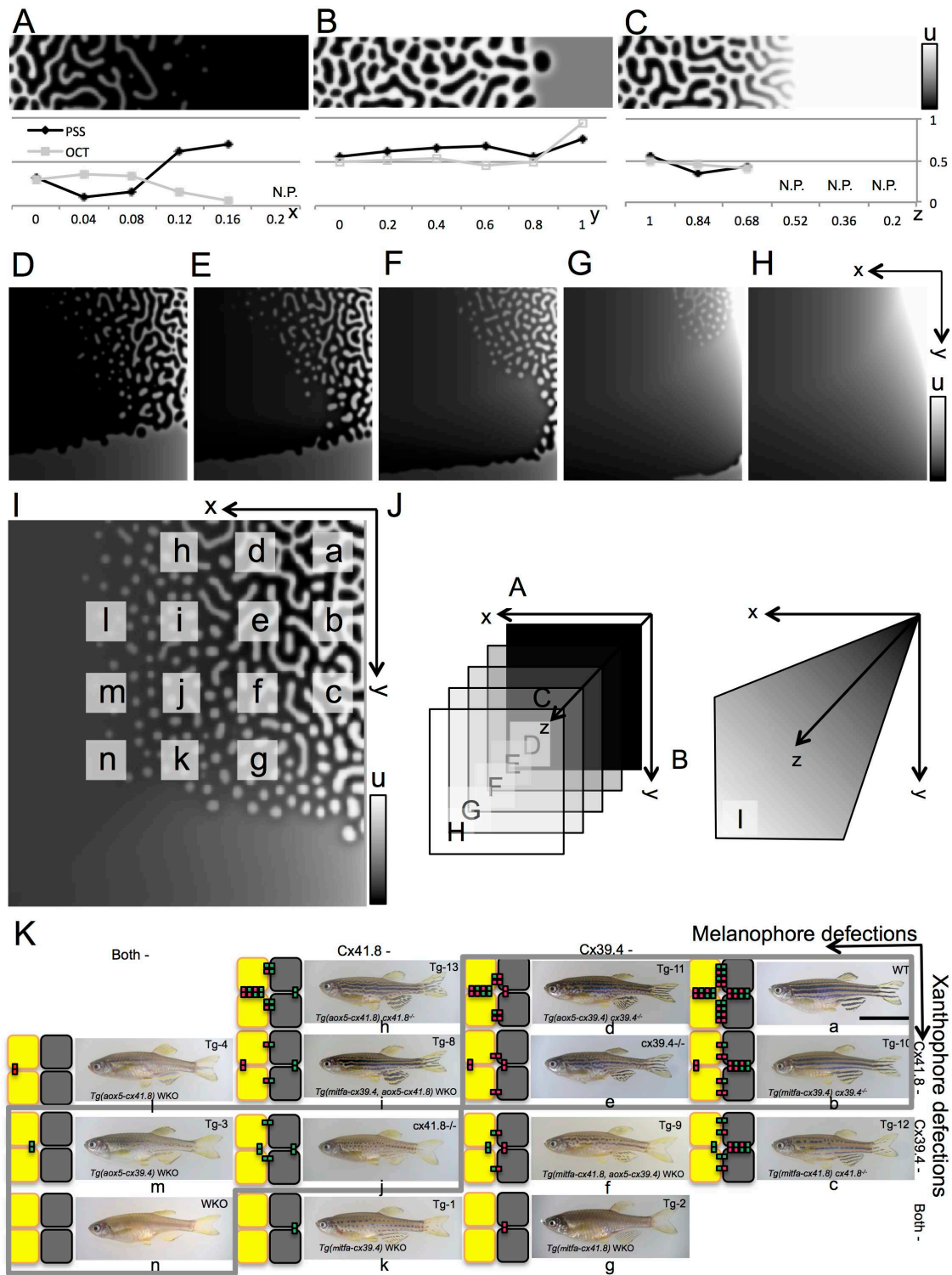
5 distributed complementarily and the highly diffusible molecule W peaks at high u .



2 **Figure 3. Parameter correspondences to two-variable systems and effects on pattern**
 3 **size.**

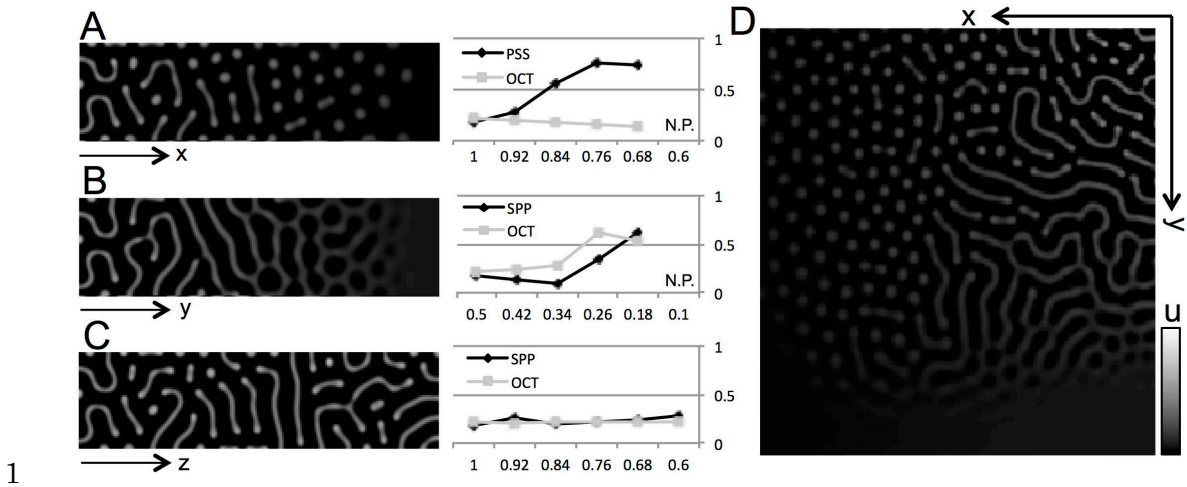
4 (A, B) Two conditions that generate a Turing pattern, activator-inhibitor type (A) or
 5 activator-substrate-depletion type (B), with different signs of reaction parameters. (C)
 6 Correspondence between parameters in the present tree-component model and the two-
 7 variable systems. Interactions included in conditions (A) and (B) are enclosed by solid and
 8 dashed polygons, respectively. (D) Matrix forms of reaction terms corresponding to the two-

- 1 variable system: the filled squares indicate the parameter that increases pattern size when
- 2 the absolute value is decreased, and the open squares denote the opposite; the solid
- 3 squares correspond to condition (A), and the dashed ones correspond to condition (B).



2 **Figure 4. Numerical results of gate effects and comparison with experiments**

1 (A)-(I) Numerical results obtained from a model of linear reaction terms with limits. Pattern
2 shifts were observed when the effects of gate defects on both cells were changed. defects
3 of gates on U and V cells, and between the cells, become larger along the x - and, y -,
4 and z (or x , y)- axes, respectively. (A)-(C) each defect was analyzed independently with
5 quantification of patterns. (A) U defect, (B) V defect, and (C) short-range defects. Pattern
6 simplicity scores (PPS) and overall color tones (OCT) were obtained quantitatively. The
7 short-range effects by gap-junctions were eliminated from arbitral wild-type condition(D)
8 0.05 to (E) 0.04, (F) 0.03, (G) 0.02, and (H) 0.01. (I) Numerical result of linear terms with
9 limits in which the short-range effects were spontaneously changed along the x - and y -
10 axes with increasing u_d and decreasing v_d . Each small letter indicates the corresponding
11 fish with connexin conditions. (J) Schematics of this analyses utilizing the present linear
12 model. U defect, (B) V defect, and (C) short-range defects were changed along with the
13 axes in each panel, as shown in the figures. (K) Pigmentation pattern on connexin-
14 manipulated fish from Usui *et al.*, 2019. Gray flamed fish had correspondence to numerical
15 results.
16



2 **Figure 5. Numerical results of gate effects by nonlinear model**

3 (A-D) Numerical results obtained from a model with nonlinear reaction terms. Pattern
 4 shifts were observed when the effects of gate defects on both cells were changed. (A) U
 5 defect, (B) V defect, and (C) short-range defects, and between the cells, became larger
 6 along the x -, y -axes, and z (or x , y)- axes, respectively. Pattern quantification by PSS
 7 and OCT are shown on the right. Then the short-range inhibitions were decreased along
 8 both axes, spontaneously. All results are shown as density plots of u .

1 **Table 1. Parameter set utilized in this paper.**

	D_u, D_v	d_u	i_{uv}	i_{uw}	s_u	i_{vu}	d_v	p_{vw}	s_v	D_w	p_{wu}	c_{wv}	d_w	s_w	min-max (for f, g)	min-max (for h)
Fig. 2 Fig.4A-D	.01	.01	.05	.05	.05	.05	.01	.05	0	1	.05	.07	.05	.02	.0 - .01	.0 - .05
Fig.4E	.01	.01	.04	.05	.05	.04	.01	.05	0	1	.05	.07	.05	.02	.0 - .01	.0 - .05
Fig.4F	.01	.01	.03	.05	.05	.03	.01	.05	0	1	.05	.07	.05	.02	.0 - .01	.0 - .05
Fig.4G	.01	.01	.02	.05	.05	.02	.01	.05	0	1	.05	.07	.05	.02	.0 - .01	.0 - .05
Fig.4H	.01	.01	.01	.05	.05	.01	.01	.05	0	1	.05	.07	.05	.02	.0 - .01	.0 - .05
Fig.5A-D	.01	+)1.	1.	1.	.2	1.	.1	1.	.5	1	1	1.	1.	.0	-	-

2